Materials Science and Engineering C 48 (2015) 287–293

Contents lists available at ScienceDirect

Materials Science and Engineering C

journal homepage: www.elsevier.com/locate/msec

Simple method for preparing glucose biosensor based on in-situ polypyrrole cross-linked chitosan/glucose oxidase/gold bionanocomposite film

Mehmet Şenel

Department of Chemistry, Faculty of Arts and Sciences, Fatih University, B.Cekmece, Istanbul 34500, Turkey

ARTICLE INFO

Article history:
Received 6 May 2014
Received in revised form 22 October 2014
Accepted 5 December 2014
Available online 9 December 2014

Keywords:
Biosensor
Glucose oxidase
Pyrrole
Immobilization
Chitosan

ABSTRACT

A film of chitosan–polypyrrole–gold nanoparticles was fabricated by in-situ chemical synthesis method and its application in glucose biosensor was investigated. The obtained biosensor exhibited a high and reproducible sensitivity of 0.58 μA/mM, response time ~4 s, linear dynamic range from 1 to 20 mM, correlation coefficient of $R^2 = 0.9981$, and limit of detection (LOD), based on S/N ratio (S/N = 3) of 0.068 mM. A value of 1.83 mM for the apparent Michaelis–Menten constant was obtained. The resulting bio-nanocomposite provided a suitable environment for the enzyme to retain its bioactivity at considerably extreme conditions, and the decorated gold nanoparticles in the bio-nanocomposite offer good affinity to enzyme.

1. Introduction

The detection of glucose level in physiological liquids such as blood and urine has an importance to make a diagnosis and treatment of diabetes mellitus. Amperometric glucose biosensors based on the glucose oxidase enzyme are more frequently employed biosensors due to its specificity [1–3]. The active site of the glucose oxidase contains two tightly bound flavin adenine dinucleotide (FAD) cofactors and catalyses the oxidation of β-D-glucose to gluconic acid, by utilizing molecular oxygen as an electron acceptor with simultaneous production hydrogen peroxide. The quantification of glucose can be achieved via electrochemical detection of the enzymatically liberated H_2O_2 [4–6].

$$\text{Glucose} + \text{GOx}\ (\text{FAD}) \rightarrow \text{GOx}\ (\text{FAD}_2) + \text{glucono lactone}$$
$$\text{GOx}\ (\text{FAD}_2) + \text{O}_2 \rightarrow \text{GOx}\ (\text{FAD}_2) + \text{H}_2\text{O}_2$$

In recent years, remarkable process in the synthesis and characterization of conducting polymers has offered a great possibility for novel applications in various fields due to considerable flexibilities in modifying their chemical structures [7,8]. By chemical modeling and synthesis, it is possible to modulate their electrical and mechanical properties [9]. Polypyrrole (PPy) is found to be of particular interest among various conducting polymers [10,11]. Conducting polymers are interesting materials for sensor and biosensor constructions due to their effective mediation of electron transfer in redox or enzymatic reactions and can be used as a suitable matrix for immobilization of biomolecules. The immobilization of desired biomolecules on the conducting polymers surface was achieved by various methods. To control over the shape and dimensions of conducting polymers by varying synthesis or processing conditions is likely to result in desired physical and electrochemical properties for biosensing application [12,13].

Chitosan is a natural polysaccharide generally obtained by the deacetylation of the natural chitin [14]. Due to its excellent biocompatibility, nontoxicity, cheapness, easy-handling and high mechanical strength, chitosan (Ch) has been widely used as a modifying reagent to prepare modified electrode [15]. It is preferable to maintain the high biological activity of the immobilized biomolecules and enhance the sensitivity of the sensor. To improve the properties of chitosan, the combination of chitosan with other materials such as ethylene diamine, thiourea, ferrocene, carbon nanotubes and urocanic acid was reported [16–19].

Metal nanoparticles have attracted much interest in the development of biosensors. Among all metal nanoparticles, gold nanoparticles have been widely used to construct biosensors due to their unique properties such as catalytic activities, optical properties, and biocompatibility. Gold nanoparticles dispersed onto different materials such as carbon paste electrode, self-assembled monolayer, conducting and non-conducting polymers to obtain biosensor interface [20,21]. The

E-mail address: msenel@fatih.edu.tr.

http://dx.doi.org/10.1016/j.msec.2014.12.020
0928-4931/

stabilization of gold nanoparticles with chitosan has been extensively studied [22]. For the composite of polymer and gold nanoparticles various monomers and polymers could be chosen. Chitosan can be adsorbed onto the surface of the gold nanoparticles due its positively charged structure and protection of gold nanoparticles [23]. In a previous study, gold nanoparticles electrochemically deposited on chitosan layer and immobilize GOx effectively [24]. Also, gold nanoparticles prepared simple chemical reduction process by using pyrrole monomer to construct biosensor through simple one-step process [25,26]. Herein, the reduction ability of the pyrrole monomer is used to prepare gold nanoparticles.

This work proposed a simple method for immobilization of GOx by using pyrrole branched chitosan as host material for enzyme and reducing agent for the formation of gold nanoparticles. Due to the distinct advantages of the PPy, chitosan and the Au nanoparticles one by one, the Chi-Py/Au cross-linked nanocomposite designed in this work for highly sensitive and stable amperometric biosensor, in which the sensing film could benefit from the good conductivity, and the superior stability and conductivity of Au nanoparticles.

2. Experimental

2.1. Materials and apparatus

Glucose oxidase (GOx) (EC 1.1.3.4), 1-ethyl-3-(3-dimethylaminopropyl)carbodiimide hydrochloride (EDC) and 1-(2-cyanoethyl)pyrrole (Py-CN) were obtained from Aldrich Chemical Co. All other chemicals were of analytical grade and used without further purification.

The FTIR-ATR measurements (4000–400 cm^{-1}) were recorded with a Bruker spectrometer. 64 spectra in the range of 4000–400 cm^{-1} were recorded with a resolution of 1 cm^{-1} and averaged. ^{1}H NMR spectra were recorded at room temperature in $CDCl_3$ (containing 0.03% tetramethylsilane as an internal reference $\delta = 0.00$ ppm) on Bruker 400 MHz spectrometer at 300 or 400 MHz.

X-ray powder diffraction (XRD) analysis was performed on a Rigaku SmartLab Diffractometer operated at 40 kV and 35 mA using Cu Kα radiation. Ch-Py, Chi-Py/Au and Chi-Py/Au/GOx layers prepared on glass slides and used for measurements of XRD.

Electrochemical impedance spectroscopy (EIS) measurements were carried out using a CHI Model 6005 electrochemical analyzer in a background solution of 5 mM Fe^{3+}/Fe^{2+} phosphate buffer (pH 7.0) at a normal potential. The alternating voltage was 5 mV and the frequency range was 5.0×10^{-2} to 1.0×10^{6} Hz.

All amperometric measurements were carried out at room temperature in stirred solutions by applying the desired potential and allowing the steady state current to be reached. Once prepared, the GOx electrodes were immersed in 10 ml of 10 mM PBS solution at pH 7.5 and the amperometric response to the addition of a known amount of glucose solution was recorded. Data collected with freshly prepared enzyme electrodes refer to the average of three experiments.

2.2. Synthesis of 1-(2-carboxyethyl)pyrrole (PyPA)

1-(2-Carboxyethyl)pyrrole was obtained by hydrolysis of 1-(2-cyanoethyl)pyrrole (Py-CN) according to literature [27]: a mixture of 25 g of Py-CN and 100 ml of 15% potassium hydroxide solution was stirred at 50 °C for 40 h. Then the mixture was cooled to room temperature and acidified by hydrochloric acid. After extraction with ether, the crude product (colorless crystals) was collected on evaporation of ether. The product was dissolved in ether and purified by recrystallization from the ether solution. The product was identified as 1-(2-carboxyethyl)pyrrole by means of FTIR-ATR, ^{1}H, and ^{13}C NMR spectroscopy (not shown).

2.3. Preparation of pyrrole branched-chitosan and enzyme electrode

The pyrrole-branched-chitosan was prepared by the formation of amide linkages through the EDC-mediated reaction following the similar method of Liu et al. [28] as shown in Fig. 1A. 1 g of chitosan was dissolved in 100 ml acetic acid solution (1% w/v) and diluted with 85 mL of methanol. PyPA was added to the chitosan solution at 0.54 mol/mol glucosamine residue of chitosan followed by a dropwise addition of 15 mL methanol solution of EDC (0.07 g/L) while stirring at room temperature. The 1:1 mole ratio of EDC to PyPA was used in this study. After 24 h, the reaction mixture was poured into 200 mL of methanol/ammonia solution (7/3, v/v) with stirring. The crude product was filtered, washed with distilled water, methanol, and ether, and then dried under vacuum for 24 h at room temperature.

The Chi-Py/Au/GOx bionanocomposite biosensor electrodes were prepared by mixing 2.5 μl of 0.0925 M Chi-Py, 10 mg/ml GOx and 2.5 μl of 0.0125 M $HAuCl_4$ solutions (in 100 mM PB pH 6.5) onto the electrode surface, respectively (Fig. 1B). The mixture on the GCE allows reacting and drying for 30 min. The electrode was then thoroughly rinsed with distilled water before use.

3. Results and discussion

3.1. Spectroscopic characterization of pyrrole branched-chitosan and gold-nanobiocomposite

The FT-IR spectra of chitosan, PyPA and pyrrole branched-chitosan are shown in Fig. 2A. Characteristic peaks of pyrrole at 1495 cm^{-1} and 1090 cm^{-1} in pure PyPA and pyrrole branched-chitosan, these have

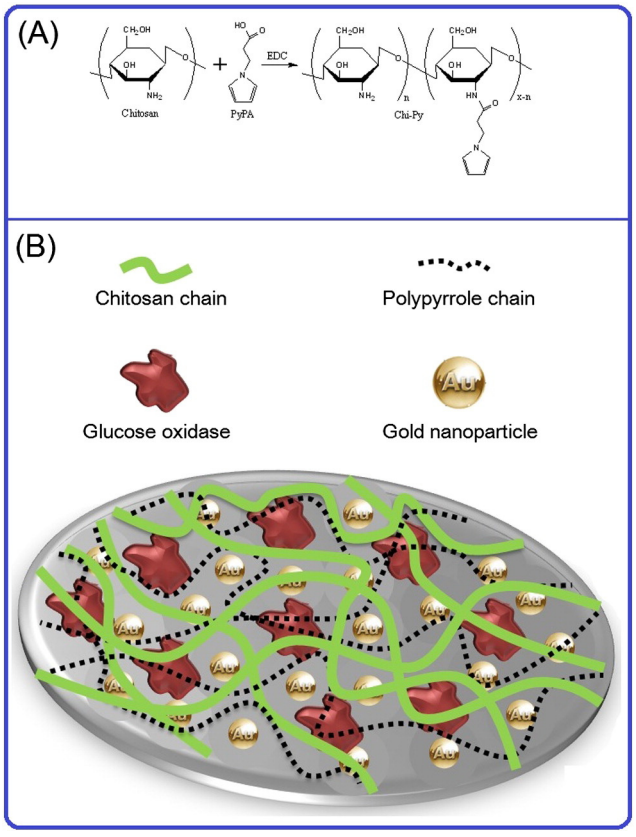

Fig. 1. A) Synthesis of pyrrole branched-chitosan. B) Schematization of the surface of GOx immobilized gold electrode.

been assigned to C═C stretching mode and C–C stretching of pyrrole ring, respectively [29]. Furthermore, chitosan and pyrrole branched-chitosan all contained the –CONH– group. The carbonyl absorption band, C═O, is known as the amide I band, and N–H is termed the amide II band. Their position depends on the degree of hydrogen bonding and, thus, the physical state of the compound. The most significant IR frequencies of the chitosan and pyrrole branched-chitosan are the amide I band (carbonyl stretching) and the amide II band (N–H deformation mode) vibration [30]. The characteristic features of the pyrrole–alginate spectrum are strong sharp peaks at 1642 and 1580 cm^{-1} which correspond to the amide I band, C═O stretching vibrations, and amide II band, N–H bending vibrations, respectively, and a medium-sharp peak at 1257 cm^{-1} (amide II band, interaction between the N–H bending and C–N stretching vibrations).

Phase investigation of the crystallized product synthesized via Chi-Py/Au method and Chi-Py precursor was performed by XRD and the diffraction pattern is presented in Fig. 2B. Due to the polymeric nature of both chitosan and pyrrole, their XRD powder patterns represent their amorphous structure. The XRD pattern indicates that the product is Au. All of the observed diffraction peaks are indexed, as presented, by the cubic structure of Au revealing a high phase purity of product agreeing with those reported for Au (JCPDS card number 101-0056) (Fig. 2B). The line profile, shown in Fig. 2B was fitted for observed 4 peaks with the following miller indices: (111), (200), (220), and (311) The average crystallite size of the product, D and σ, was 15 ± 6 because of this line profile fitting.

Branching of chitosan with pyrrole was also confirmed by a ^1H NMR spectroscopy, and the ^1H NMR spectra of Chi-Py are shown in Fig. 2C. The signals at δ 1.95, 2.68, 3.09 − 3.70 and 4.70 ppm were assigned to the resonance of the monosaccharide residue protons [31]. The signals appearing at δ 6.02–6.72 ppm in the ^1H NMR spectra of Chi-Py attributed to the pyrrole ring protons, and they revealed that a couple of the pyrrole residue to the chitosan could be achieved via coupling agent-mediated reaction.

3.2. Morphological characterization

Scanning electron microscope microphotographs of the surfaces of Chi-Py, Chi-Py/Au and Chi-Py/Au/GOx are shown in Fig. 3. Compared with the surface of Chi-Py, the Chi-Py/Au nanocomposite with uniform granular morphology was attributed to the formation of Au nanoparticles. It demonstrated that during the chemical polymerization process of pyrrole group of chitosan gold nanoparticles were formed in chitosan membrane. The granular porous surface of the Chi-Py/Au nanocomposite film is suitable for the immobilization of biomolecules. As GOx is immobilized into the Chi-Py/Au nanocomposite matrix the morphology of the Chi-Py/Au surface changes to the well-regulated form. The surface of GOx immobilized Chi-Py/Au nanocomposite changes when GOx is immobilized into the Chi-Py/Au nanocomposite matrix.

3.3. Electrochemical characterization of modified electrode

Electrochemical characterizations of bare GCE, GCE/Chi-Py and GCE/Chi-Py/Au nanocomposite coated electrodes were carried out by cyclic voltammetry (CV), as shown in Fig. 4A. CVs were

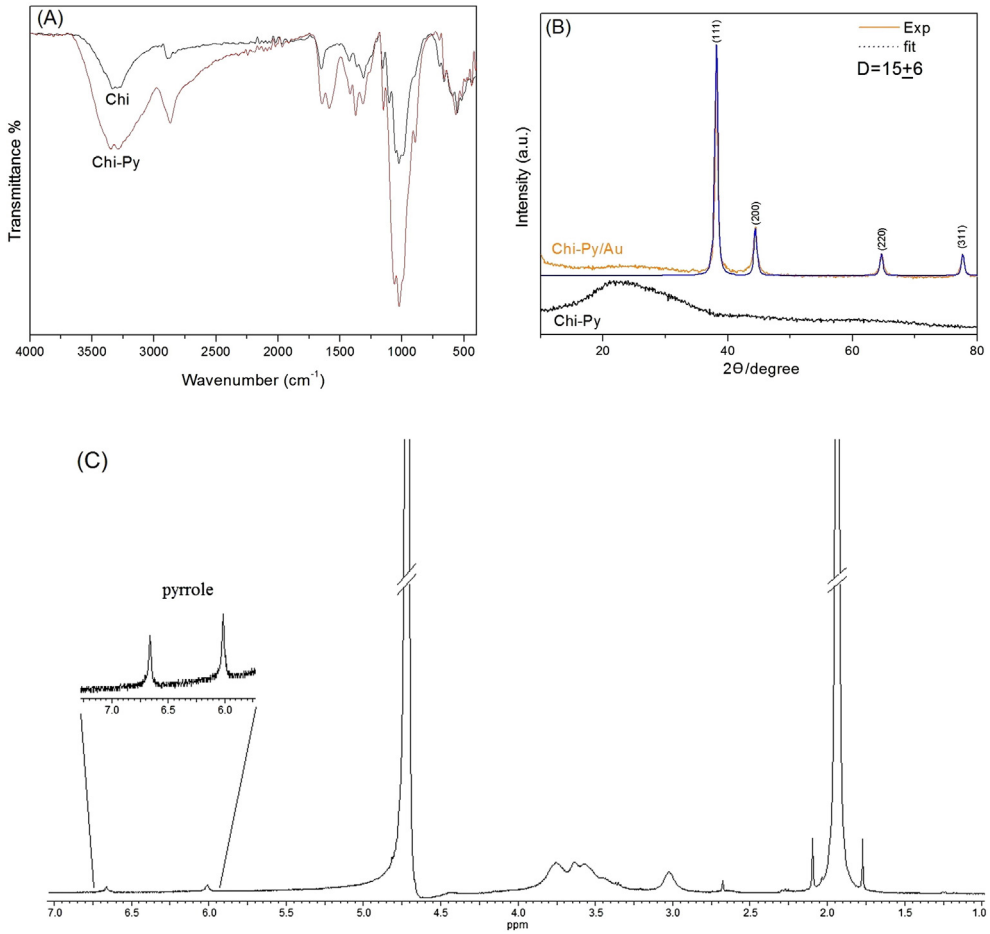

Fig. 2. A) FTIR-ATR spectra of chitosan (Chi), pure PyAA and pyrrole branched-chitosan (Chi-Py). B) X-ray diffraction patterns of chitosan–pyrrole (Chi-Py) and Chi-Py/Au. C) ^1H-NMR spectra of Chi-Py in D_2O containing 5% CD_3COOD.

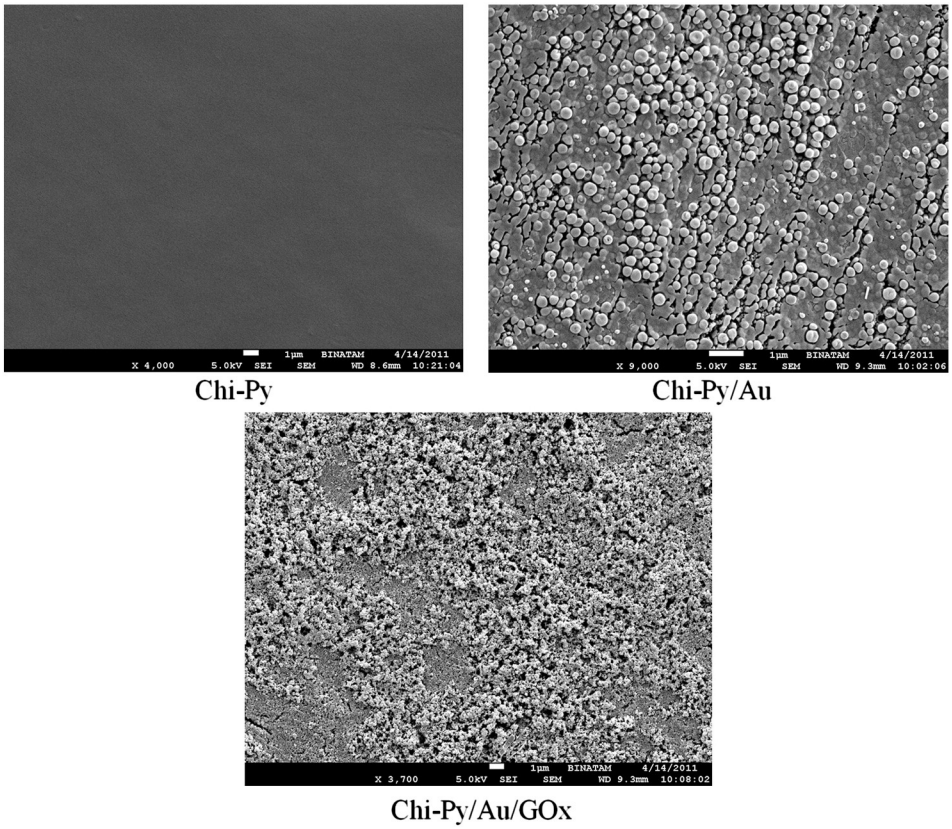

Fig. 3. Scanning electron microscopic (SEM) micrographs of Chi-Py, Chi-Py/Au and Chi-Py/Au/GOx (magnification; ×4000, ×9000 and ×3700, respectively).

performed in 5 mM $Fe^{II}(CN)_6^{4-}/Fe^{III}(CN)_6^{3-}$ as a model reversible redox couple at potential range of −0.2 to 0.7 V versus Ag/AgCl at a scan rate of 100 mV/s. As shown in Fig. 4A, the response of redox couple at the GCE/Chi-Py/Au (curve c) is much stronger than that at GCE/Chi-Py (curve b). This enhanced electrochemical behavior is attributed to the presence of gold nanoparticles in the polymeric film [32,33]. For further characterization, cyclic voltammograms of (a) bare GCE, (b) GCE/Chi-Py and (c) GCE/Chi-Py/Au electrodes in 100 mM PB solution, pH 7.5 were performed (Fig. 4B). An oxidation peak at 1.12 V was shown for the GCE–PPyPA–Au electrode and attributed to the oxidation of Au^0 to Au^{3+} in the form of Au_2O_3 [34]. This result confirmed that the presence of gold nanoparticles in the Chi-Py film deposited on the surface of the electrode.

Electrochemical impedance spectroscopy (EIS) is an effective technique to demonstrate the interfacial properties of modified electrode and often used for understanding electrochemical transformations and processes associated with the conductive supports [35]. The semicircular part, included in EIS curves, at higher frequencies corresponds to the electron-transfer-limited process and its diameter is equal to the electron transfer resistance, which controls the electron transfer kinetics of the redox probe at the electrode interface [36]. Fig. 4C shows that the electron transfer resistance decreases in the order of the modified electrodes: bare GCE < GCE/Chi-Py/Au < GCE/Chi-Py, which indicates that the Au nanoparticles improve the conductivity of the composite film-modified GCE. Both the EIS and CV results reveal that the Chi-Py/Au nanocomposites can be incorporated into the electrochemical system to improve electron transfer and facilitate the electron transfer between the electrode and the enzyme due to enhanced conductivity of the matrices.

3.4. Optimization of experimental variables of biosensor

The applied potential has a strong effect on the biosensor responses because it contributes to the sensitivity and selectivity of the biosensor. The effect of the applied potential on the response of the biosensor electrode was determined and the results are shown in Fig. 5A. The biosensor response to glucose solution increased with the change of the applied potential. It is shown that the current of glucose addition increases until a potential of 0.4 V. To obtain the highest current response in the amperometric measurements and decrease the interference effects, therefore the working potential was selected to be 0.4 V.

The influence of the pH of supporting electrolyte over the range of 5.0–9.0 on the amperometric response of the biosensor to glucose in PBS was also investigated. The results show that the optimum pH was 7.0 (Fig. 5B). This pH value is used for further amperometric measurements.

In addition, the effect of the temperature on the amperometric response of the biosensor to glucose was investigated in the range of 25–60 °C, which was showed in Fig. 5C. The response increased with an increase of the temperature and reached a maximum at 50 °C, and then the response decreased. The denaturation of GOx or instability of the films in high temperatures might cause it.

3.5. Determination of glucose at modified electrode

The typical steady-state amperometric response of the biosensor was investigated by successively increasing the glucose concentration under the optimized conditions. Fig. 6 shows the amperometric curve

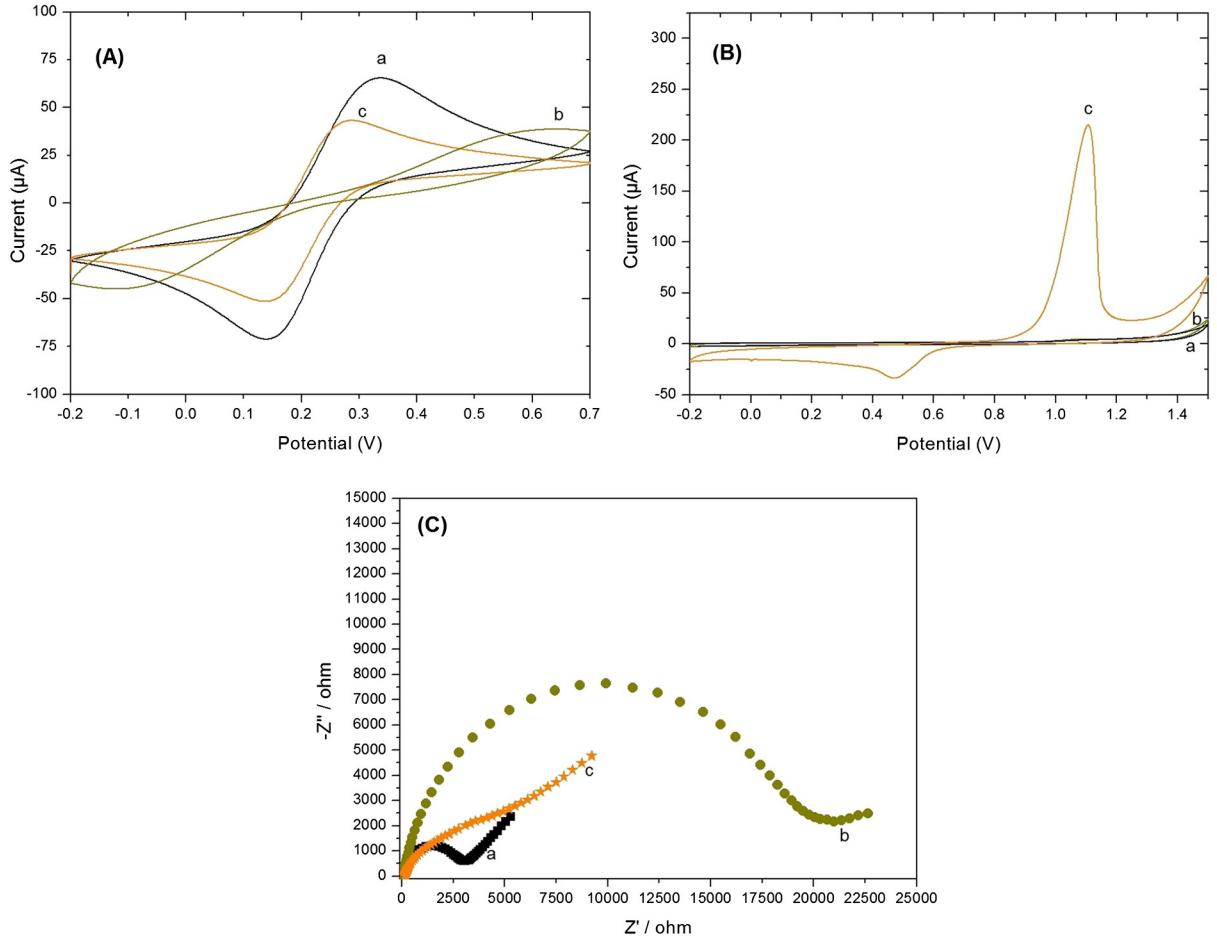

Fig. 4. A) Cyclic voltammograms of (a) bare GCE, (b) GCE/Chi-Py and (c) GCE/Chi-Py/Au electrodes in 10 mM PBS solution, pH 7.0 containing $[Fe(CN)_6]^{3-/4-}$ (5 mM). B) Cyclic voltammograms of (a) bare GCE, (b) GCE/Chi-Py and (c) GCE/Chi-Py/Au electrodes in 100 mM PB solution, pH 7.0. C) Electrochemical impedance spectra of (a) bare GCE, (b) GCE/Chi-Py and (c) GCE/Chi-Py/Au electrodes in 10 mM PBS solution, pH 7.0 containing $[Fe(CN)_6]^{3-/4-}$ (5 mM).

of the biosensor for successive addition of glucose solution with stirring. The enzyme electrode exhibited a rapid response to the chance of substrate concentration and reached steady-state current with-in ~4 s. The effect of the nanoparticles on the biosensor performance for glucose detection was compared in Fig. 6 and the GCE/Chi-Py/Au/GOx electrode shows four times higher response than the GCE/Chi-Py/GOx electrode. This result showed that the incorporation of Au nanoparticles in chitosan film increased the efficiency of the biosensor. The inset of Fig. 6 shows the calibration curve between amperometric current and glucose concentration. An excellent linear relationship was obtained in the concentration range 1.0 to 20.0 mM with correlation coefficient of 0.9987. The detection limit of this biosensor was estimated as 0.068 mM at a signal-to-noise ratio of three. The sensitivity of the biosensor was found as 0.58 μA/mM. The apparent Michaelis–Menten constant K_m^{app} is an indicator of the enzyme–substrate reaction kinetics and is used to evaluate the biological activity of the immobilized enzyme. According to the Lineweaver–Burk form of the Michaelis–Menten equation, the relationship between the response current and the glucose concentration is obtained as follows:

$$\frac{1}{I_{ss}} = \frac{K_m^{app}}{I_{max}\ C} + \frac{I}{I_{max}}$$

where I_{ss} is the steady-state response current after the addition of substrate; I_{max} is the maximum response current under saturated substrate conditions; and C is the bulk concentration of glucose. The K_m^{app} value of the glucose biosensor was found as 4.34 mM which was little smaller than the previous study [37] for GOx immobilized on the electrode surface. The smaller K_m^{app} value means that the immobilized GOx possesses higher enzymatic activity.

3.6. Stability, reusability, interference and sample analysis studies

Both storage stability and operational stability are important from the practical application point of view, so these two parameters were examined. The reusability features of glucose biosensor were investigated by performing measurements in a definite time scale (Fig. 7A). The response of glucose biosensor gave relatively closed results for first ten measurements, and activity loss 55% was observed with further application. The storage stability of the biosensor was examined over a 50-day period (Fig. 7B). When the biosensor was stored in a refrigerator at 4 °C and measured intermittently, after 50 days of storage, the biosensor retained about 67% of its original response.

In addition, the influences of common interfering electroactive substances in the analysis of plasma samples were studied at + 0.4 V versus Ag/AgCl in pH 7.0 phosphate buffer and presented in Fig. 7C. The interference tests were carried with three common interfering compounds: ascorbic acid, acetaminophen and uric acid, respectively. The interfering effects of adding 0.5 mM uric acid (UA), 0.1 mM acetaminophen (AA)

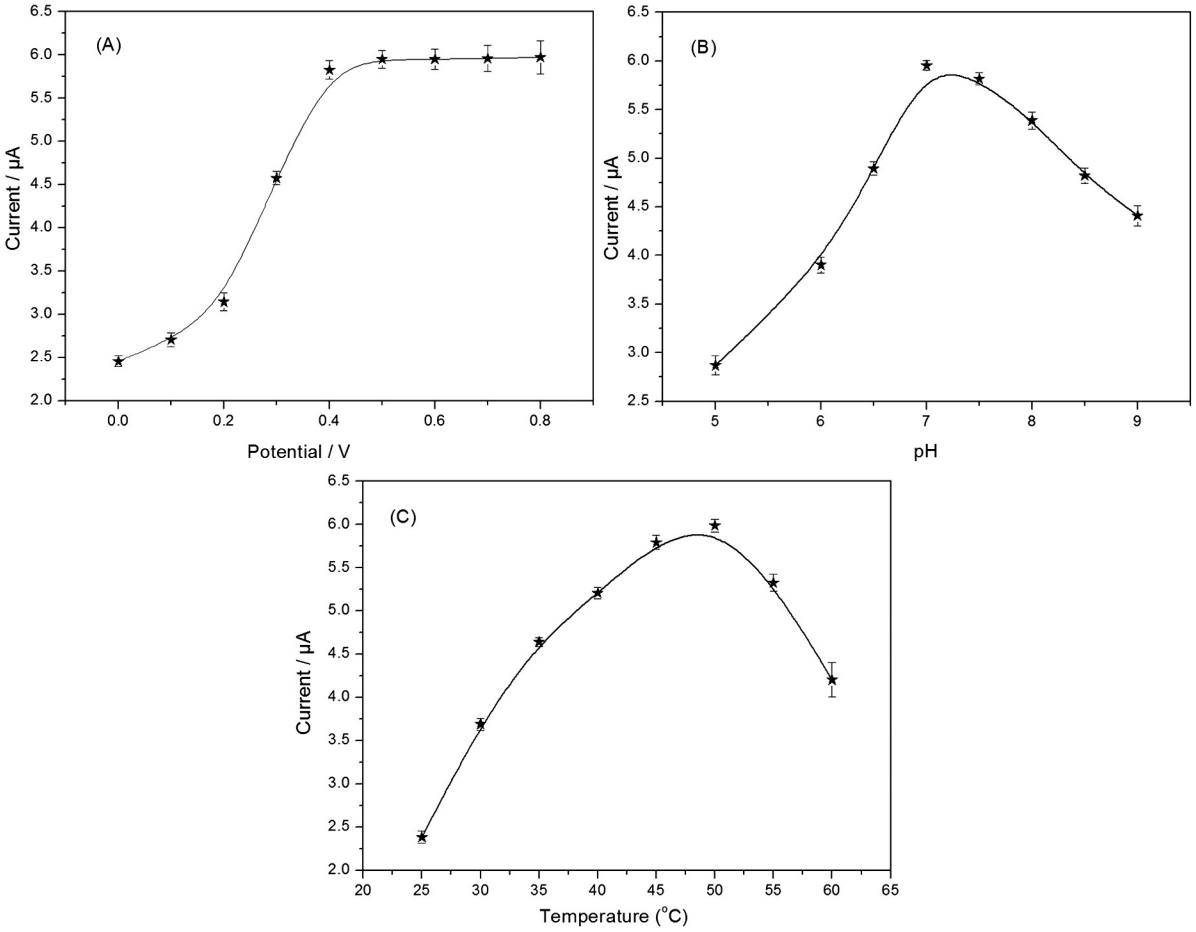

Fig. 5. A) Effect of potential on the current response of the GOx immobilized electrodes by addition of 10 mM glucose at various levels of applied potential in 10 M PBS (pH 7.5 and ~25 °C), B) Effect of pH on GOx immobilized electrodes in 10 M PBS (~25 °C) and C) effect of temperature on GOx immobilized electrodes in 10 M PBS (pH 7.5).

and 0.1 mM ascorbic acid (AsA) are nearly eliminated at the enzyme electrode, compared to the high sensitivity of the result glucose biosensor, the interference current can be negligible similar as the previous studies [38].

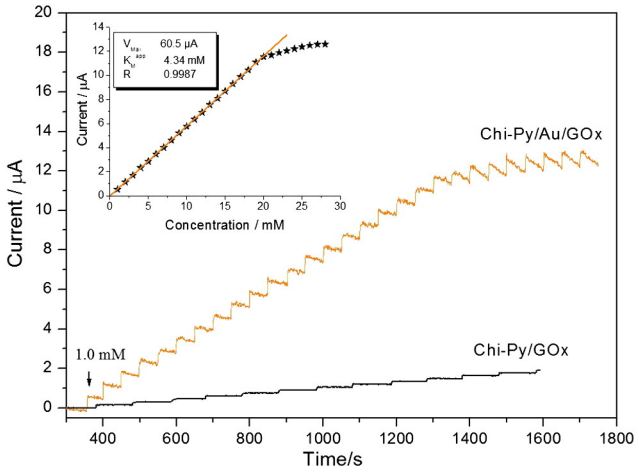

Fig. 6. Amperometric response of enzyme electrodes to successive glucose solution (1 mM) injections at an applied potential +0.4 V in stirred 10 mM PBS (pH 7.0). The inset shows the calibration curve.

The determination of glucose in human serum samples was performed with the prepared biosensor. Biochemical automatic analyzer in local hospital assayed the serum samples at the same time. A plasma sample (1.0 ml) was added into 5 ml PBS (pH 7.0), and the response was obtained at constant potential (+0.4 V). The glucose content of the blood plasma can then be calculated from the calibration plot of the enzyme electrode. The results were shown in Table 1. The glucose levels determined in this work were close to the values declared by hospital, indicating that the fabricated glucose biosensor has practical potential.

4. Conclusions

This study describes a facile method for the fabrication of chitosan–polypyrrole–gold nanocomposite film using pyrrole-branched chitosan and $HAuCl_4$. The resulted nanocomposite film containing chemically formed gold nanoparticles can be used to entrap glucose oxidase. After immobilizing the glucose oxidase into the nanocomposite film modified Au electrode, a new amperometric glucose biosensor has been successfully developed. The glucose biosensor shows good analytical characteristics such as a short response time, high sensitivity, lower detection limit and good stability under the optimized experimental conditions. The film fabrication technique demonstrated in this work and its application on biosensor are readily applicable to the fabrication of other chitosan–conducting polymer–metal nanoparticles film and biosensors based on biomaterials.

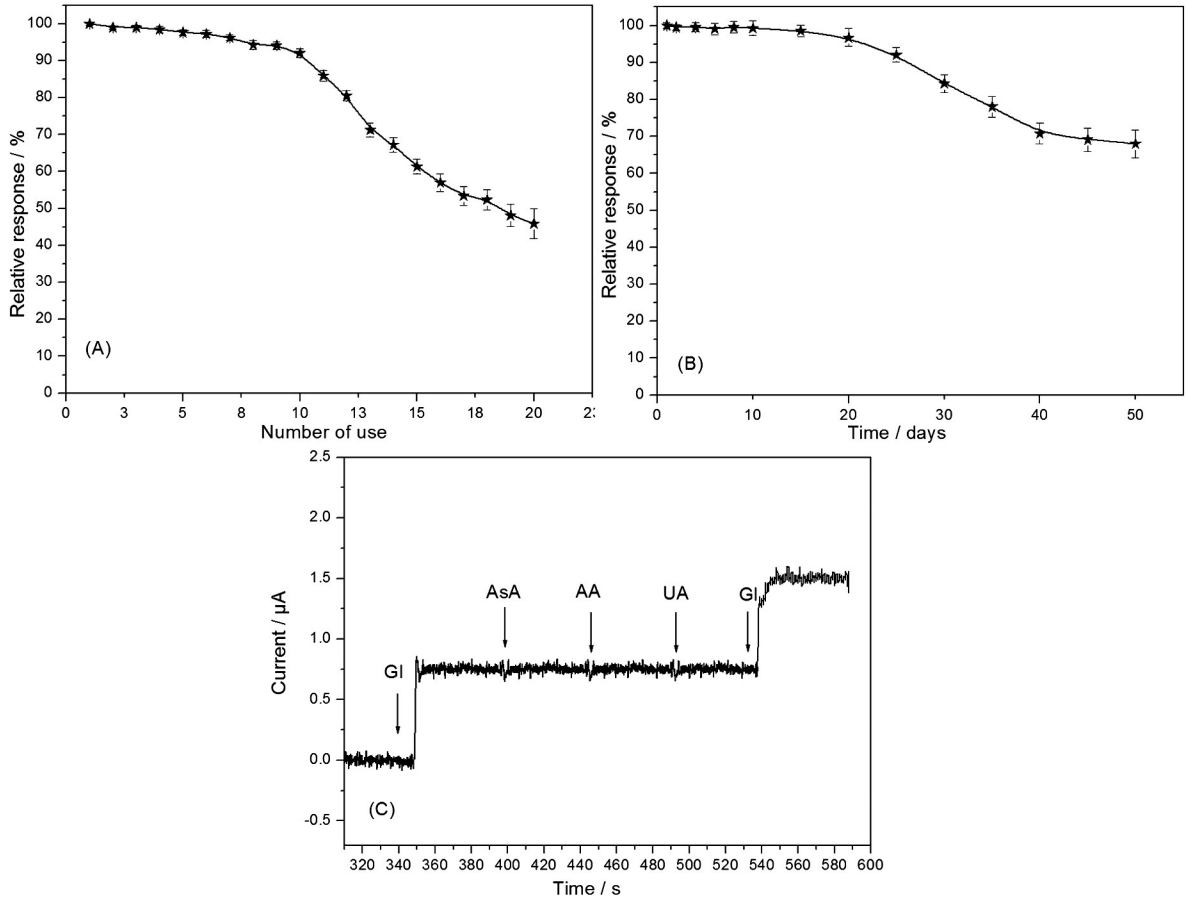

Fig. 7. A) Reusability of glucose biosensor (pH 7.5; ~25 °C). B) Long-time stability of GOx immobilized electrode. The amperometric responses of these enzyme electrodes are regularly checked during 50 days by adding 4 mM glucose solution (pH 7.5; ~25 °C). C) Current-time response curve for the enzyme electrode obtained on subsequent additions of 0.1 mM ascorbic acid (AsA), 0.1 mM acetaminophen (AA), 0.5 mM uric acid (UA) and 1 mM glucose (Gl).

Table 1
Glucose content determination in serum samples.

Samples	Determined by Hospital (mM)	Measured by biosensor (mM)*	RSD (%)	Relative error (%)
1	5.51	5.38 ± 0.22	4.0	−2.36
2	4.85	4.93 ± 0.07	1.4	+1.86
3	5.24	5.32 ± 0.22	4.0	+1.53

* Average of the three measurements.

References

[1] L. Xinyu, Z. Yunlong, Z. Zhaozhu, Y. Xiuli, D. Zhifei, L. Shaoqin, T. Zhiyong, Langmuir 25 (2009) 6580–6586.
[2] W. Yu-Ho, Seong J. Ho, M.K. Seung, S. Eric, G. Mallikarjunarao, A. Silvana, A.S. Lia, Langmuir 26 (2010) 4320–4326.
[3] S.D. Bryan, D.D. Jonathan, Anal. Biochem. 375 (2008) 132–140.
[4] Z. Dai, Z. Ke, L.Y. Yan, H.X. Xing, Y.C. Hong, Langmuir 20 (2004) 7303–7307.
[5] Z. Guanghong, X. Yibo, G. Jian, W. Zhiqiang, Z. Xi, Langmuir 26 (2010) 15022–15026.
[6] M. Piano, S. Serban, N. Biddle, R. Pittson, G.A. Drago, J.P. Hart, Anal. Biochem. 396 (2010) 269–274.
[7] Y. Yoon, J. Jang, Adv. Funct. Mater. 19 (2009) 1567–1576.
[8] J. Jang, Adv. Polym. Sci. 199 (2006) 189–190.
[9] Zarini Muhammad Tahi, Evangelyn C. Alocilja, Daniel L. Grooms, Biosens. Bioelectron. 20 (2005) 1690–1695.
[10] A. Kumar, A. Rajesh, S.K. Chaubey, B.D. Grover, J. Malhotra, Appl. Polym. Sci. 82 (2001) 3486–3491.
[11] Suman Singh, Asha Chaubey, B.D. Malhotra, Anal. Chim. Acta. 502 (2004) 229–234.
[12] A. Kumar, Rajesh, A. Chaubey, S.K. Grover, B.D. Malhotra, J. Appl. Polym. Sci. 82 (2001) 3486–3491.
[13] S. Singh, A. Chaubey, B.D. Malhotra, 229–234, Anal. Chim. Acta. (2004) 502.
[14] O.E. Philippova, E.V. Volkov, M.L. Sitnikova, A.R. Khokhlov, J. Desbrieres, M. Rinaudo, Biomacromolecules 2 (2001) 483–490.
[15] X.L. Luo, J.J. Xu, Q. Zhang, G.J. Yang, H.Y. Chen, Biosens. Bioelectron. 21 (2005) 190–196.
[16] R.K. Katarina, T. Takayanagi, M. Oshima, S. Motomizu, Anal. Chim. Acta. 558 (2006) 246–253.
[17] O.B. Mokhodoeva, G.V. Myasoedova, I.V. Kubrakova, J. Anal. Chem. 62 (2007) 607–622.
[18] T.H. Kim, J.E. Ihm, Y.J. Choi, J.W. Nah, C.S. Cho, J. Control. Release 93 (2003) 389–402.
[19] J. Hodak, R. Etchenique, E.J. Calvo, K. Singhal, P.N. Bartlett, Langmuir 13 (1997) 2708–2716.
[20] N. Rosi, C. Mirkin, Chem. Rev. 105 (2005) 1547–1562.
[21] M. Daniel, D. Astruc, Chem. Rev. 104 (2004) 293–346.
[22] D.S. dos Santos Jr., P.J.G. Goulet, N.P.W. Pieczonka, O.N. Oliveira Jr., R.F. Aroca, Langmuir 20 (2004) 10273–10277.
[23] H. Huang, X. Yang, Colloids Surf. A 226 (2003) 77.
[24] Du. Ying, Xi-Liang Luo, Jing-Juan Xu, Hong-Yuan Chen, Bioelectrochemistry 70 (2007) 342–347.
[25] J. Njagi, S. Andreescu, Biosens. Bioelectron. 23 (2007) 168–175.
[26] M. Senel, C. Nergiz, Curr. Appl. Phys. 12 (2012) 1118–1124.
[27] S.E. Wolowacz, B.F.Y. Yon-Hin, C.R. Lowe, Anal. Chem. 64 (1992) 1541–1545.
[28] C.G. Liu, K.G.H. Desai, X.G. Chen, H.J. Park, J. Agric, Food Chem. 53 (2005) 437–441.
[29] İ. Bozgeyik, M. Senel, E. Cevik, M.F. Abasıyanık, Curr. Appl. Phys. 11 (2011) 1083–1088.
[30] Shu-Jyuan Yang, Feng-Huei Lin, Kun-Che Tsai, Ming-Feng Wei, Han-Min Tsai, Jau-Min Wong, Ming-Jium Shieh, Bioconjug. Chem. 21 (2010) 679–689.
[31] Peggy Chan, Motoichi Kurisawa, Joo Eun Chung, Yi-Yan Yang, Biomaterials 28 (2007) 540–549.
[32] J.M. Pingarron, P. Yáñez-Sedeño, A. González-Cortés, Electrochim. Acta 53 (2008) 5848–5866.
[33] J. Kim, J.W. Grate, P. Wang, Chem. Eng. Sci. 61 (2006) 1017–1026.
[34] L.D. Burke, P.F. Nugent, Gold Bull. 30 (1997) 43–53.
[35] Liqiang Luo, Qiuxia Li, Xu. Yanhong, Yaping Ding, Xia Wang, Dongmei Deng, Yinjuan Xu, Sensors Actuators B Chem. 145 (2010) 293–298.
[36] S.F. Yardimci, M. Senel, A. Baykal, Mater. Sci. Eng. C 32 (2012) 269–275.
[37] M. Senel, Synth. Met. 161 (2011) 1861–1868.
[38] B. Zheng, S. Xie, L. Qian, H. Yuan, D. Xiao, M.M.F. Choi, Sensors Actuators B 152 (2011) 49–55.